Advances in Nano Research, *Vol. 16, No. 4 (2024) 341-352*
https://doi.org/10.12989/anr.2024.16.4.341

Numerical and statistical analysis of Newtonian/non-Newtonian traits of MoS_2-$C_2H_6O_2$ nanofluids with variable fluid properties

Manoj C Kumar[a] and Jasmine A Benazir[*]

Department of Mathematics, Presidency university, Bengaluru, Karnataka, India

(*Received September 27, 2023, Revised December 29, 2023, Accepted February 21, 2024*)

Abstract. This study investigates the heat and mass transfer characteristics of a MoS_2 nanoparticle suspension in ethylene glycol over a porous stretching sheet. MoS_2 nanoparticles are known for their exceptional thermal and chemical stability which makes it convenient for enhancing the energy and mass transport properties of base fluids. Ethylene glycol, a common coolant in various industrial applications is utilized as the suspending medium due to its superior heat transfer properties. The effects of variable thermal conductivity, variable mass diffusivity, thermal radiation and thermophoresis which are crucial parameters in affecting the transport phenomena of nanofluids are taken into consideration. The governing partial differential equations representing the conservation of momentum, energy, and concentration are reduced to a set of nonlinear ordinary differential equations using appropriate similarity transformations. R software and MATLAB-bvp5c are used to compute the solutions. The impact of key parameters, including the nanoparticle volume fraction, magnetic field, Prandtl number, and thermophoresis parameter on the flow, heat and mass transfer rates is systematically examined. The study reveals that the presence of MoS_2 nanoparticles curbs the friction between the fluid and the solid boundary. Moreover, the variable thermal conductivity controls the rate of heat transfer and variable mass diffusivity regulates the rate of mass transfer. The numerical and statistical results computed are mutually justified via tables. The results obtained from this investigation provide valuable insights into the design and optimization of systems involving nanofluid-based heat and mass transfer processes, such as solar collectors, chemical reactors, and heat exchangers. Furthermore, the findings contribute to a deeper understanding of stretching sheet systems, such as in manufacturing processes involving continuous casting or polymer film production. The incorporation of MoS_2-$C_2H_6O_2$ nanofluids can potentially optimize temperature distribution and fluid dynamics.

Keywords: MHD; MoS_2-$C_2H_6O_2$ nanofluids; Sisko fluid model; variable mass diffusivity; variable thermal conductivity

1. Introduction

In recent years, there has been a growing interest in exploring the thermal and fluidic behavior of nanoparticle suspensions for various industrial and engineering applications scrutinized by (Cui *et al.* 2022, Choi and Eastman 1995, Shah *et al.* 2022a, b, Sidik *et al.* 2015, Selmi 2019, Kobayashi *et al.* 2013, Nagaraj *et al.* 2023, Pavitra *et al.* 2023, Sur 2014). The study of heat and mass transfer characteristics of nanofluids, particularly those containing innovative nanomaterials like MoS_2 (Molybdenum Disulfide), has garnered significant attention in various heat exchange systems due to their exceptional thermal and mechanical properties. It can be used at temperatures ranging from -600 °C to 400 °C. It is known as the "king of solid lubricants" because it can be lubricated in a vacuum or air environment for a longer duration. It is a hexagonal crystal with a layered structure stacked by S-Mo-S in alternating layers, as shown in Fig. 1.1. China is the largest country in MoS_2 resources with reserves of 4.3 million tons. The ethylene glycol is considered a base fluid because it is known for its excellent heat transfer properties and widespread use as a coolant. As demonstrated in Fig. 1.2, the heat and mass transfer behavior of MoS_2 nanoparticle suspension in ethylene glycol over a stretching sheet offers promising applications in the biomedical and engineering domains examined by (Pourmadadi *et al.* 2022, Bazaka *et al.* 2019, Liu *et al.* 2021, Abd-Elkader *et al.* 2023, Shah and Awan 2022, Zhang *et al.* 2015, Saidi *et al.* 2021, Ahmed *et al.* 2022, Bas 2023, Mousavi *et al.* 2020). Some biomedical applications include: In healing therapies, it can be adapted to model the temperature and moisture distribution of wound dressings to inhibit bacterial growth. In photothermal therapy, these nanocomposites when selectively generate localized heat which can effectively destroys the cancer cells or tumors. This suspension can be used to create biocompatible coatings on medical implants and devices to reduce the risk of rejection by the body. MoS_2-$C_2H_6O_2$ nanoparticle suspensions also hold significant promise in various engineering applications. MoS_2 nanoparticles dispersed in ethylene glycol create a nanofluid that provides better heat transfer characteristics that can cool electronic components and devices with high power densities. Additionally, this lubricant reduces the friction and wear of bearings and gears in mechanical systems, leading to enhanced efficiency and longevity. These versatile suspensions also find merit in aerospace engineering. The high-temperature stability and lubricating properties of these materials can enhance the performance and durability of spacecraft and gas turbine engines, thereby extending the reach of materials engineering

*Corresponding author, Ph.D.,
E-mail: jasminebenazir@gmail.com
[a] Ph.D., E-mail: mngowda9676@gmail.com

ISSN: 2287-237X (Print), 2287-2388 (Online)

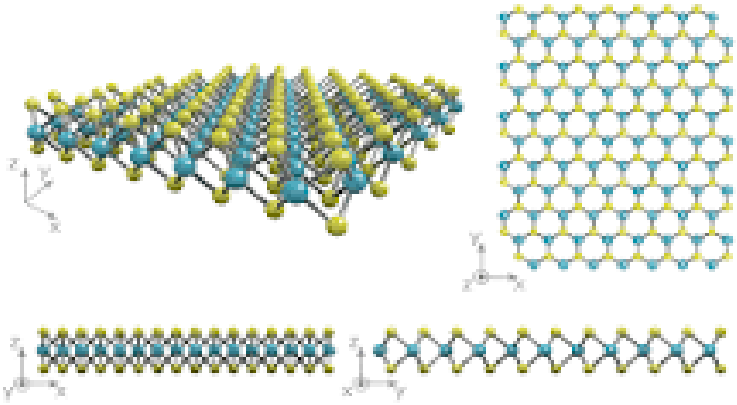

Fig. 1.1. Structural representation of MoS_2

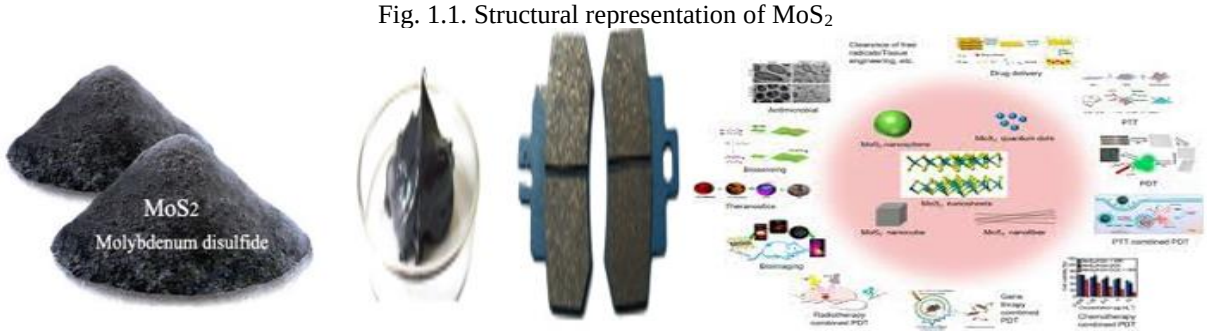

Fig. 1.2 Applications of MoS_2

into diverse industries. MHD and porous medium are essential concepts in the study of flow and heat transfer analysis. However, electrical conducting nanofluids flow over a porous medium have significant applications in the science and engineering such as design of MHD generators, soil remediation, material processing, oil and gas industries, etc. Numerous researchers studied the transport behavior of MHD and porous medium (Choudhary and Jain 2021, Gharseldien and Awaad 2022, Huang *et al.* 2022, Liu *et al.* 2023, Maalla and Song 2021, Safari *et al.* 2021, Sharif *et al.* 2021a, b, 2023, Ali *et al.* 2022)

The variable thermal conductivity and variable mass diffusion are important aspects to consider in the context of energy and mass distribution of nanofluids flow over a porous medium. It is an important factor encountered in fluid mechanics and materials processing; particularly in metal formation. During these processes, the quality of the metal product primarily depends on the extent of heat and mass transfer. Variable thermal conductivity influences the temperature distribution across the stretching sheet. As the sheet is stretched, the temperature dependent thermal conductivity causes the local temperature gradients to change causing non-uniform heat distribution in the material. This affects the structural integrity of the sheet and makes it equipped for heat-related processes such as drying and annealing. Variable mass diffusion is crucial when dealing with species transport on a stretching sheet. Different substances may diffuse at different rates through the material or the fluid boundary layer near the sheet. In applications like chemical vapor deposition or coating processes, variations in mass diffusion coefficients can significantly affect the uniformity and quality of the deposited layers. Additionally, in biological systems such as tissue engineering and drug delivery devices, it plays a pivotal role in controlling the distribution of nutrients and chemicals. This impacts the growth and functionality of tissues and the effectiveness of drug delivery systems. In many industrial applications, the management of Newtonian and non-Newtonian nanofluids with variable mass diffusivity and variable thermal conductivity is essential for optimization and guaranteeing the design and product quality (Algehyne *et al.* 2022, Alsenafi *et al.* 2021, Sohail *et al.* 2020, Amirsom *et al.* 2019, Rashed *et al.* 2021, Sivaraj *et al.* 2019).

The study of non-Newtonian nanofluids represents a fascinating topic in fluid dynamics and nanomaterial science, ushering in a new era of understanding fluid behavior at the nanoscale. Unlike traditional Newtonian fluids, non-Newtonian fluids deviate from linear viscosity patterns exhibiting intricate rheological complexities influenced by factors such as shear rate and temperature. When these fluids are incorporated with nanoparticles the resulting nanofluids offers a dynamic and unique set of challenges and opportunities. Various fluid models such as Maxwell fluid model, Oldroyd-B fluid model, Williamson fluid model, Sisko fluid model, Casson fluid model, etc. have been developed to analyze the non-Newtonian fluid behaviors (Razzaq *et al.* 2021a, b, c2022, Awan *et al.* 2022a, b). In this context, Sisko model is an extension of the classical Newtonian fluid model which accommodates the non-Newtonian characteristics often exhibited by nanofluids, especially at higher particle concentrations. This trait of Sisko fluid is utilized for the current analysis. The shear-thinning behavior and yield stress of the Sisko model

offers a more accurate representation of the complex rheological properties inherited by nanoparticle suspensions. There are numerous studies that have reported the rheological transport features in Sisko nanofluids (Pal and Mandal 2019, Jan *et al*. 2022, Raju and Sandeep 2016, Waqas *et al*. 2022, Bisht and Maheshwari 2023, Khan and Shahzad 2013).

From the crucial literature survey, one of the key manufacturing techniques for developing components for domestic purpose, automotive, and aerospace applications is sheet metal forming. The quality of the components formed by this process depends extensively on the extent of lubrication provided between the dyes and forming surfaces. The effective lubrication during the process can be achieved by using solid lubricants such MoS_2 which can bear the huge impact loads and can also provide a media for heat dissipation during the frictional heating of the dye and the forming surface. MoS_2 nanoparticles with their unique lubricating and anti-friction properties can be dispersed in $C_2H_6O_2$ to form nanofluids for sheet metal applications to enhance heat transfer characteristics and reduce frictional losses. Hence considering the above facts, the stretching sheet is modeled with the mathematical assumptions highlighted in problem formulation section.

This investigation intricately explores the numerical computation of heat and mass transfer phenomena of nanofluid (MoS_2-$C_2H_6O_2$) flow over elongating porous sheet using the Sisko fluid model. The effects of variable thermal conductivity, variable mass diffusivity, thermal radiation, thermophoresis and chemical reactions are taken into account as they are crucial parameters affecting the transport phenomena of nanofluids. The governing partial differential equations representing the conservation of momentum, energy, and concentration are reduced to a set of nonlinear ordinary differential equations using appropriate similarity transformations. R software and MATLAB-bvp5c are used to compute the solutions. From this systematic investigation, the current research provides deeper insights into the heat - mass transfer and flow patterns that govern the behavior of these nanofluids.

2. Problem formulations

The stretching sheet has been accelerated with uniform velocity $U_w = cx$ along the horizontal direction, where c is the non-negative real number. A uniform magnetic field B_0 is applied perpendicular to the surface and Darcy porous medium is taken in to account. The energy and concentration equations are explored with the mechanism of variable thermal conductivity, variable mass diffusivity of nano-particle and its base fluids, thermal radiation, thermo-phoresis and 1st - order chemical reactions. The surface of the stretching sheet is maintained at a constant temperature T_w and constant concentration C_w. In addition, T_∞ and C_∞ are free stream temperature and free stream concentration, respectively. The Joule and viscous dissipation are assumed to be negligibly small. The values of thermophysical properties of nanoparticles and base fluids are given in Table 1 The characteristics equations to obtain the thermo-physical properties of nanofluids is given in Appendix section.

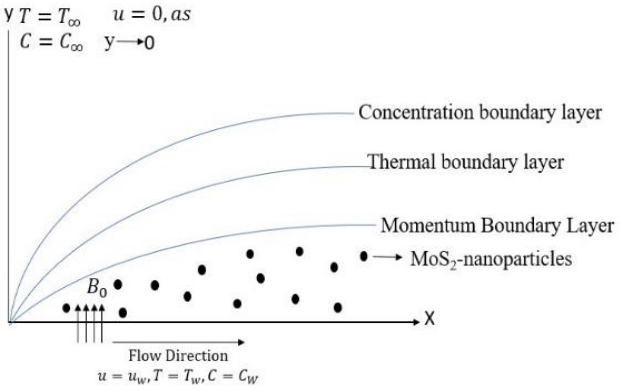

Fig. 2 Geometry of the flow problem

Table 1 The values of thermophysical property parameters of MoS_2 and $C_2H_6O_2$ (Ganesh *et al*. 2019, Hamid *et al.* 2021, Hussain 2022)

Physical Properties	Fluid Phase ($C_2H_6O_2$)	MoS_2
ρ(Kg/m^3)	1116.6	5.06× 10^3
k(W/mK)	0.249	904.4
C_p(J/kgK)	2382	397.21
$\sigma(\Omega/m)^{-1}$	1.07× 10^{-7}	2.09× 10^{-4}
P_r	200.9	-

Based on above stated assumptions, the boundary layer flow of the governing equations is described as follows.

$$\frac{\partial u}{\partial x} + \frac{\partial v}{\partial y} = 0 \tag{1}$$

$$u\frac{\partial u}{\partial x} + v\frac{\partial u}{\partial y} = \frac{a_{nf}}{\rho_{nf}}\frac{\partial^2 u}{\partial y^2} - \frac{b}{\rho_{nf}}\frac{\partial}{\partial y}\left(-\frac{\partial u}{\partial y}\right)^n - \frac{\sigma B_0^2 u}{\rho_{nf}} - \frac{\mu}{\rho_{nf}K}u \tag{2}$$

$$u\frac{\partial T}{\partial x} + v\frac{\partial T}{\partial y} = \frac{1}{(\rho c_p)_{nf}}\frac{\partial}{\partial y}\left[k_{nf}(T)\left(\frac{\partial T}{\partial y}\right)\right] - \frac{1}{(\rho c_p)_{nf}}\left(\frac{\partial q_r}{\partial y}\right) + \tau\left[\begin{matrix}\left(\frac{\partial}{\partial y}\left[D_{B,\infty}(C - C_\infty)\right]\right) \\ \left(\frac{\partial T}{\partial y}\right) + \frac{D_T}{T_\infty}\left(\frac{\partial T}{\partial y}\right)^2\end{matrix}\right] \tag{3}$$

$$u\frac{\partial C}{\partial x} + v\frac{\partial C}{\partial y} = \frac{\partial}{\partial y}\left[D_{B,\infty}(C)\frac{\partial C}{\partial y}\right] + \frac{D_T}{T_\infty}\frac{\partial^2 T}{\partial y^2} - K_r(C - C_\infty) \tag{4}$$

The appropriate boundary constraints for the Eqs. (1)-(4) are as follows:

$$U_w = cx, v = 0, T = T_w, C = C_w \; at \; y = 0 \tag{5}$$

$$u \to 0, T \to T_\infty, C \to C_\infty \; at \; y \to \infty \tag{6}$$

Using (Rosseland 1931) approximation, the thermal radiation is written as $q_r = -\frac{4\sigma^*}{3k^*}\frac{\partial T^4}{\partial y}$

The variable thermal conductivity and nanoparticles diffusivity are assumed in the form of (Alsenafi *et al*. 2021, Sohail *et al*. 2020).

$$k_{nf}(\theta) = k_\infty(1+\varepsilon\theta)$$
$$D_B(\chi) = D_{B_\infty}(1+\varepsilon_1\chi)$$

where ε and ε_1 are small variable thermal conductivity and nanoparticle diffusivity parameters respectively.

For mathematical analysis of the problem, the following similarity transformations are used to convert the P.D.Es to O.D.Es

$$\begin{aligned} u &= cxf'(\eta),\\ v &= -u_w Re_b^{-\frac{1}{n+1}}\frac{1}{n+1}[2nf(\eta)+(1-n)\eta f'(\eta)],\\ \eta &= \frac{y}{x}Re_b^{\frac{1}{n+1}}\\ \theta(\eta) &= \frac{T-T_\infty}{T_w-T_\infty}, \chi(\eta) = \frac{C-C_\infty}{C_w-C_\infty} \end{aligned} \tag{7}$$

Substituting Eq. (7) in Eqs. (1)-(4), the following non-dimensional coupled differential equations are obtained:

$$\begin{aligned} &a_1 Af'''(\eta) + n\big(-f''(\eta)\big)^{(n-1)}f'''(\eta)\\ &-a_3 Mf'(\eta) - a_2(f'(\eta))^2 + a_2\frac{2n}{n+1}f(\eta)f''(\eta)\\ &-D_a f'(\eta) = 0 \end{aligned} \tag{8}$$

$$\begin{aligned} &\frac{a_4}{a_5}\big(1+R+\varepsilon\theta(\eta)\big)\theta''(\eta) + \varepsilon\theta'(\eta)^2 + P_r\frac{2n}{n+1}f(\eta)\theta'(\eta)\\ &+\frac{1}{a_5}\Big[N_B\theta'(\eta)\chi'(\eta)[1+2\varepsilon_1\chi(\eta)] + N_T\big(\theta'(\eta)\big)^2\Big] = 0 \end{aligned} \tag{9}$$

$$\begin{aligned} &[1+2\varepsilon_1\chi(\eta)]\chi''(\eta) + \varepsilon_1\big(\chi'(\eta)\big)^2 + \frac{N_T}{N_B}\theta''(\eta)\\ &-LeP_r\left(-\frac{2n}{n+1}f(\eta)\chi'(\eta) + \sigma\chi(\eta)\right) = 0 \end{aligned} \tag{10}$$

The appropriate boundary conditions of Eqs. (8) – (10) are followed by

$$f(0) = 0,\ f'(0) = 1,\ \theta(0) = 1,\ \chi(0) = 1\ at\ \eta = 0 \tag{11}$$

$$f'(\infty)\to 0, \theta(\infty)\to 0, \chi(\infty)\to 0\ at\ \eta\to\infty \tag{12}$$

where the non-dimensional parameters are,

$$\begin{aligned} &A = \frac{Re_b^{\frac{2}{n+1}}}{Re_a},\ M = \frac{{B_0}^2\sigma}{c\rho_{nf}}, D_a = \frac{\nu_{nf}}{Kc},\\ &P_r = \frac{xu_w}{\alpha Re_b^{\frac{2}{n+1}}}, R = \frac{16\sigma^* T_\infty^3}{3k_{nf_\infty}k^*}, Re_a = \frac{\rho_{nf}xu_w}{a},\\ &Re_b = \frac{\rho_{nf}x^n{u_w}^{2-n}}{b}, N_B = \frac{\tau D_{B,\infty}}{\alpha}(C_w - C_\infty),\\ &\alpha = \frac{k_{nf_\infty}}{\rho_{nf c_p}}, N_T = \frac{\tau D_T}{\alpha T_\infty}(T_w - T_\infty), \sigma = \frac{K_r}{c}, L_e = \frac{\alpha}{D_{B,\infty}} \end{aligned} \tag{13}$$

The dimensionless physical quantities of interest are the local skin friction coefficient C_{fx}, the local Nusselt number Nu_x, the local Sherwood number Sh_x which are mathematically denoted as:

$$\begin{aligned} &C_{fx} = \frac{2\tau_w}{\rho{u_w}^2}, Nu_x = \frac{xq_w|_{y=0}}{K(T)(T_w - T_\infty)}\\ &Sh_x = \frac{xj_w|_{y=0}}{D_B(C)(C_w - C_\infty)} \end{aligned} \tag{14}$$

The stress tensor(τ_w), heat flux (q_w) and mass flux (j_w) are defined as

$$\begin{aligned} &\tau_w = \left(a - b\left|-\frac{\partial u}{\partial y}\right|^{n-1}\right), q_w = -K(T)\left(\frac{\partial T}{\partial y}\right),\\ &j_w = -D_B(C)\left(\frac{\partial C}{\partial y}\right) \end{aligned} \tag{15}$$

Using Eq. (7), the output of solutions of dimensionless physical quantities are shown below

$$\frac{1}{2}Re_b^{\frac{1}{n+1}}C_{fx} = \frac{1}{(1-\Phi)^{2.5}}\big(Af''(0) - \big(-f''(0)\big)^n\big) \tag{16}$$

$$Re_b^{-\frac{1}{n+1}}Nu_x = -\frac{K_{nf}}{K_f}\big(\theta'(0)\big) \tag{17}$$

$$Re_b^{-\frac{1}{n+1}}Sh_x = -\chi'(0) \tag{18}$$

3. Solution methodology

Obtaining an exact solution for the non-linear coupled boundary value problem is highly challenging. To address this difficulty, the governing equations from Eqs. (8)-(10) along with their corresponding boundary conditions Eqs. (11)-(12) are solved numerically. This is achieved through the application of the four-stage Lobatto IIIa formula using MATLAB bvp5c function by incorporating suitable initial approximations. The problem cannot be tackled on an infinite interval, and even solving it over a very large finite interval is not practical. To address this, an artificial boundary condition of bvp5c is introduced at a finite point η, with a discretization step size of h=0.0505, simulating the behavior at infinity. Within this framework, the four-stage Lobatto IIIa formula is characterized as a collocation technique and is implemented via the finite difference code bvp5c. This method ensures C^1-continuity and attains fifth-order accuracy in the solution. Additionally, the formula is executed as an implicit Runge-Kutta (R.K.) method. To facilitate the solution process, the governing equations are transformed into a set of first-order differential equations by introducing new variables.

$$f = f_1, f' = f_2, f'' = f_3, \theta = f_4, \theta' = f_5, \chi = f_6, \chi' = f_7$$

$$\begin{aligned} f_3' = -\frac{1}{(a_1 A + n(-f_3)^{(n-1)})}\Big[&-a_3 Mf_2 - a_2(f_2)^2\\ &+ a_2\frac{2n}{n+1}f_1 f_3 - D_a f_2\Big] \end{aligned} \tag{19}$$

$$\begin{aligned} f_5' = -\frac{1}{\frac{a_4}{a_5}(1+R+\varepsilon f_4)}\Big[&\varepsilon f_5^2 + P_r\frac{2n}{n+1}f_1 f_5\\ &+\frac{1}{a_5}[N_B f_5 f_7[1+2\varepsilon_1 f_6] + N_T f_5']\Big] \end{aligned} \tag{20}$$

$$f_7' = -\frac{1}{(1+2\varepsilon_1 f_6)}\left[\varepsilon_1 f_7^2 + \frac{N_T}{N_B} f'_5 - LeP_r\left(-\frac{2n}{n+1} f_1 f_7 + \sigma f_6\right)\right] \quad (21)$$

The associated boundary conditions are as follows:

$$f_1 = 0,\ f_2 = 1,\ f_4 = 1,\ f_6 = 1,\ at\ \eta = 0 \quad (22)$$

$$f_2 \to 0, f_4 \to 0, f_6 \to 0\ at\ \eta \to \infty \quad (23)$$

4. Result and discussions

The ensuing discussion unveils the intricacies of the numerical and statistical findings, providing a comprehensive understanding of the nanofluid behavior within the context of variable fluid properties. The governing Eqs. (8)-(10) along with their corresponding boundary conditions Eqs. (11)-(12) are solved numerically through MATLAB. The impact of various physical parameters on flow, heat and mass transfer characteristics are demonstrated through graphs and tables by fixing values of *A=1.5*, *M=1.5*, φ *=0.01*, P_r*=200*, *R=0.5*, N_T*=0.1*, N_B*=0.1*, σ*=0.2*, L_e*=2*, ε*=0.1*, ε_1*=0.1*. The aforementioned default values are set for the governing parameters based on the previous investigations. R software is used for computing the statistical results of engineering parameters.

The Figs. 3.1-3.4 illustrate the impact of various parameters on the velocity profile of MoS_2-$C_2H_6O_2$ for both shear thickening (solid lines, n=1.5) and shear-thinning fluid (doted lines, n=0.5) behaviors. From the figures, it is evident that shear thickening fluids flows slower than shear thinning fluids. This phenomenon makes it ideal for high lubrication. This result portrays that Shear-thinning fluids typically have a more pronounced velocity gradient compared to shear-thickening fluids. Fig. 3.1 elucidates the variation of MoS_2 volume fraction (ϕ) over the fluid velocity. As the volume fraction of MoS_2 increases, the viscosity of the fluid also increases. Higher viscous fluids tend to have a diminished velocity profile. Material parameter (A) is defined as the ratio of high shear rate viscosity to consistency index and higher values of n signify stronger shear thickening behavior. Consequently, it is observed from Fig. 3.2 that the resistance to the fluid flow decreases as the fluid moves away from the proximity of the surface for augmenting the values of the material parameter. The variation of the magnetic field in a MoS_2-$C_2H_6O_2$ suspension system can have a significant impact on the velocity profile of the fluid. When an external magnetic field is applied to such a system, it can induce MHD effects, particularly if the fluid is electrically conductive. When the strength of magnetic field rises, the Lorentz force becomes stronger and resists the fluid motion. This force hinders the fluid's ability to flow freely, leading to a reduction in its velocity profile as shown in Fig. 3.3. Variation of porous medium parameter has substantial impact on the velocity profile. Enhanced values of D_a signifies high permeability of the medium which obstructs the fluid to flow.

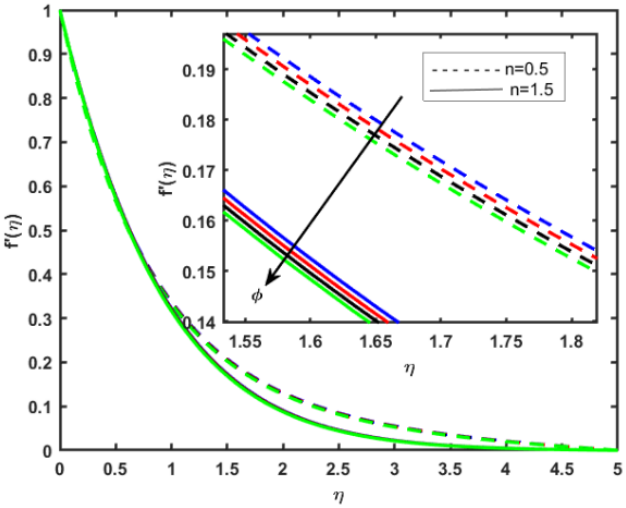

Fig. 3.1 Variation of ϕ on velocity profile

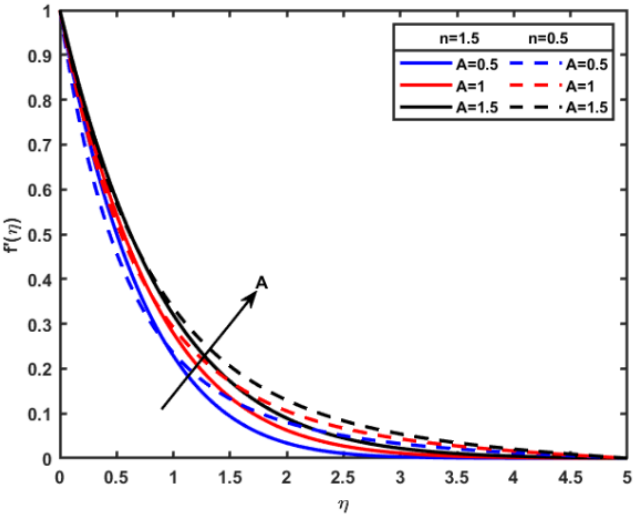

Fig. 3.2 Variation of *A* on velocity profile

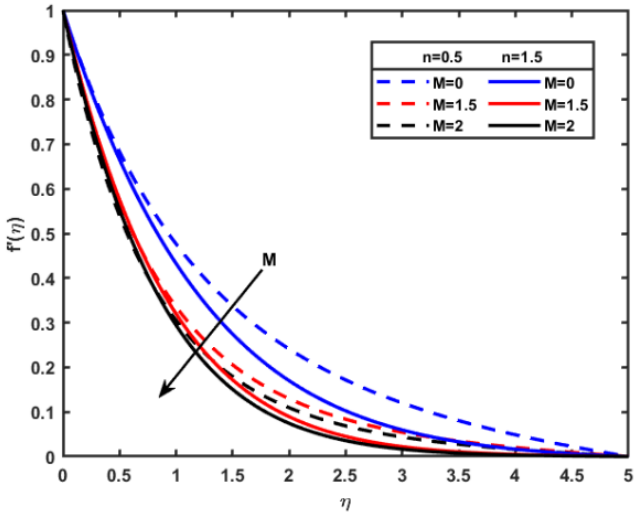

Fig. 3.3 Variation of *M* on velocity profile

Subsequently, the velocity of the fluid decreases as it encounters greater resistance as evident from Fig. 3.4. In

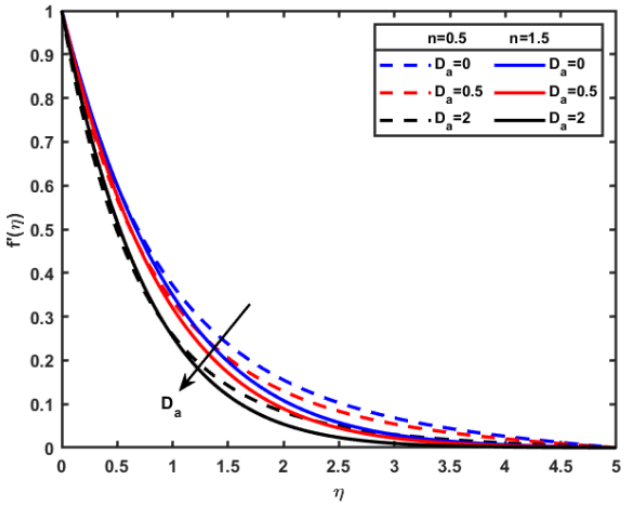

Fig. 3.4 Variation of D_a on velocity profile

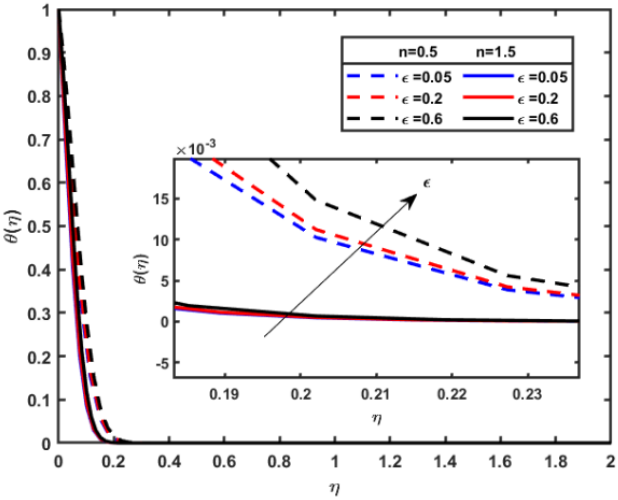

Fig. 4.3 Variation of ε on temperature profile

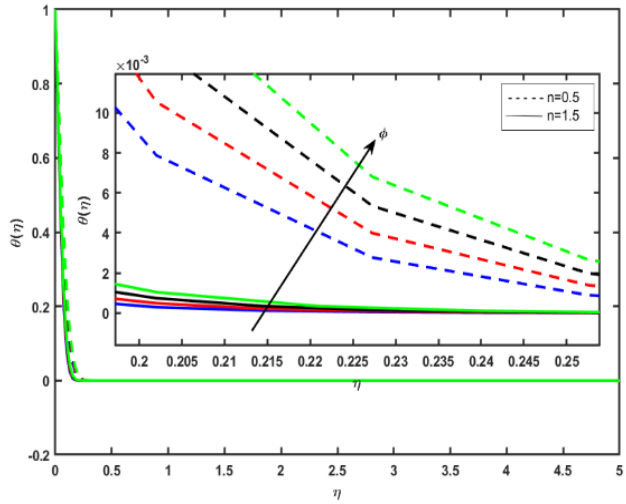

Fig. 4.1 Variation of ϕ on temperature profile

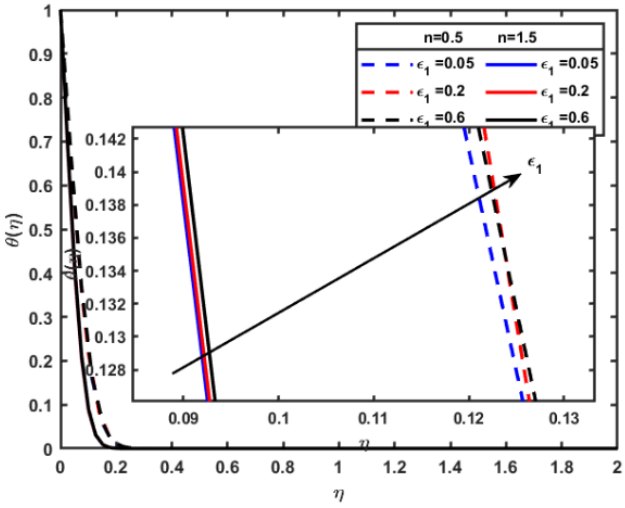

Fig. 4.4 Variation of ε_1 on temperature profile

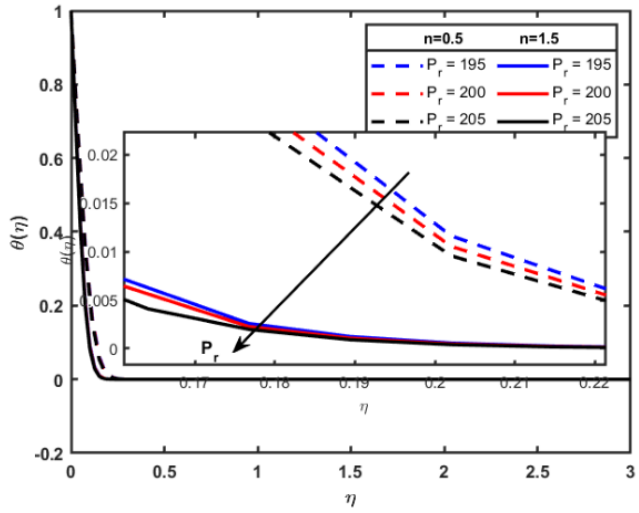

Fig. 4.2 Variation of P_r on temperature profile

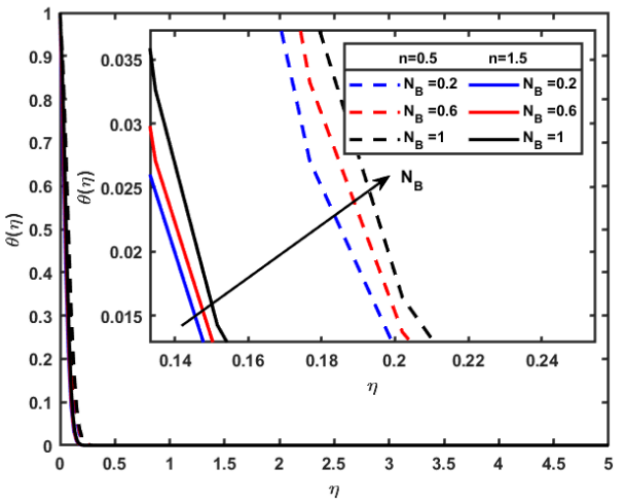

Fig. 4.5 Variation of N_B on temperature profile

general, the increased porous permeability parameter can affect the overall flow stability which in turn, potentially leads to transition from laminar to turbulent flow. Figs 4.1-4.6 portray the impact of thermal boundary layer over various parameters for both dilatant and pseudoplastic MoS_2-$C_2H_6O_2$ suspension fluids. The shear – thinning fluid

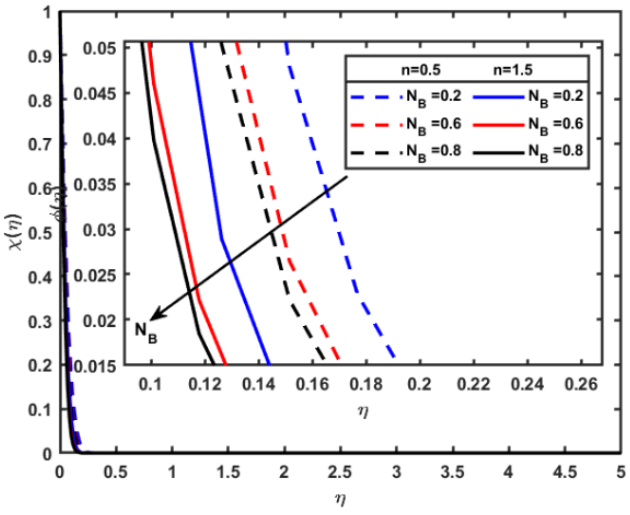

Fig. 4.6 Variation of N_T on temperature profile

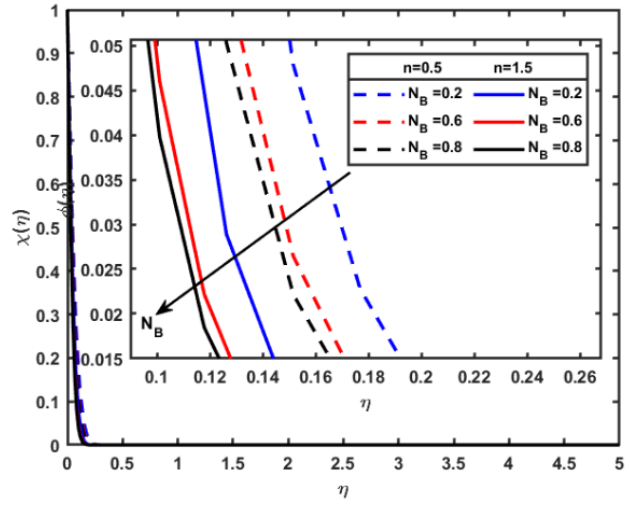

Fig. 5.1 Variation of N_B on mass transfer profile

stimulates higher thermal boundary layer as the fluid has low viscosity when it approaches the heated surface. In contrast, shear - thickening fluids exhibit reduced temperature profile because of their high viscosity. This unique property helps to maintain a relatively stable temperature making them suitable for temperature control applications. Fig 4.1 depicts the variation of volume fraction $(\phi = 0, 0.1, 0.02, 0.03)$ on nanofluid temperature profile. It is observed that the fluid temperature is enhanced for upsurging the values of ϕ. This is for the reason that MoS_2 has high thermal conductivity properties. As the volume fraction of these nanoparticles increases, so does the overall thermal conductivity of the suspension. This improvement facilitates more efficient heat transfer. In addition to this, increased nanoparticle volume fraction promotes stable and controlled temperatures, making it valuable for applications in thermal management such as in electronics cooling and heat exchangers. Fig 4.2 encapsulates that augmenting the values of Prandtl number (P_r) leads to decelerate the temperature distribution. The momentum diffusivity is more prominent than the thermal diffusivity which impedes the heat transfer. As a result, it contributes to a more controlled and stabilized temperature profile. Figs. 4. 3-4.4 exemplify that the intensifying values of variable thermal conductivity (ε) and variable mass diffusivity (ε_1) parameters in MoS_2-$C_2H_6O_2$ nanofluids result in an increase in the temperature profile due to an intensified heat conduction and mass diffusion processes. These parameters play a major role in enhancing thermal transport and mass transfer within the nanofluid. As their values rise, the nanofluid becomes more efficient at conducting heat and diffusing mass which leads to an improved temperature uniformity. This effect is particularly beneficial in applications requiring precise temperature control, such as in thermal management systems and heat exchangers. However, increased values of these parameters contribute to more stable and controlled temperature profiles.

Figs. 4.5-4.6 reveal that increasing the values of Brownian motion and thermophoresis parameters result in improved nanoparticle dispersion and heat transfer, which raises the temperature profile. These variables induce more thermophoretic and Brownian motion in nanoparticles which enhances heat conduction and dispersion throughout the nanofluid. As a result of minimal temperature gradient, a more consistent and regulated temperature profile is obtained. The heating efficiency of thermal control systems and cooling equipment can be improved by increasing the values of these parameters.

Figs. 5.1- 5.4 elucidate the significance of mass transfer of various parameters for both dilatant and pseudoplastic fluid behaviors. From all the figures, it is noted that shear thinning fluids exhibits more mass transfer compared to shear thickening fluids. Shear thinning fluids undergo better mixing and enhanced convective mass transport when subjected to shear forces, promoting efficient mass transfer. In contrast, the shear thickening fluids due to their high viscosity hinder the fluid flow and diffusion, making them less effective for mass transfer processes. The mass transfer profile decreases for increasing values of Brownian motion parameter due to enhanced nanoparticle dispersion and reduced concentration gradients. As Brownian motion becomes more apparent better dispersion of the nanoparticles is experienced due their random motion. However, this also results in more uniform nanoparticle distribution throughout the fluid leading to reduced concentration differences over the stretching sheet as shown in Fig 5.1. The mass transfer profile is enhanced for increasing values of thermophoresis parameter in MoS_2-$C_2H_6O_2$ nanofluids due to the augmented movement of nanoparticles in response to temperature gradients. The region of higher temperature attracts greater nanoparticle migration as the values of thermophoresis parameter are fostered. This concentration of nanoparticles in thermally active zones create more pronounced concentration gradients thus increasing the mass transfer which is portrayed in Fig 5.2. Strengthening the variable mass diffusion parameter upsurges the mass transfer phenomenon which is observed from Fig 5.3. This is due to fact that intensifying the variable mass diffusivity parameter

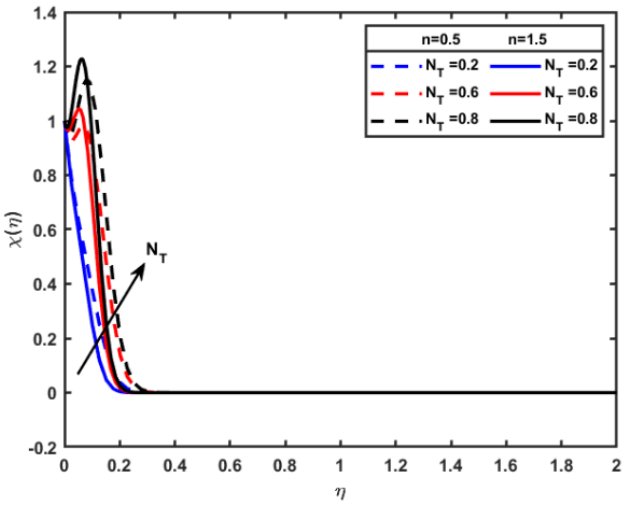

Fig. 5.2 Variation of N_T on mass transfer profile

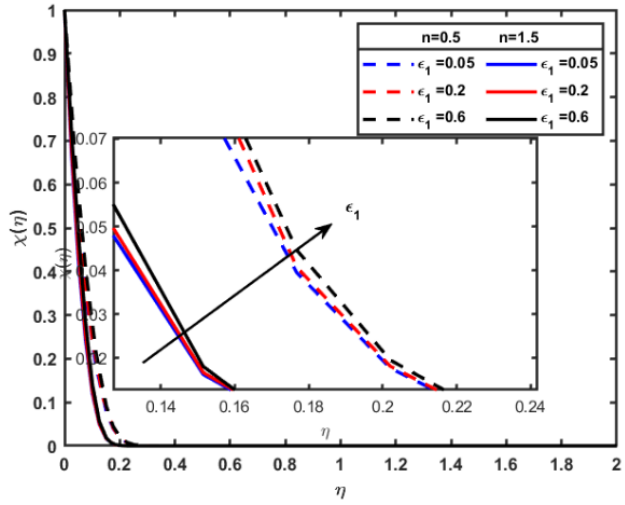

Fig. 5.3 Variation of ε_1 on mass transfer profile

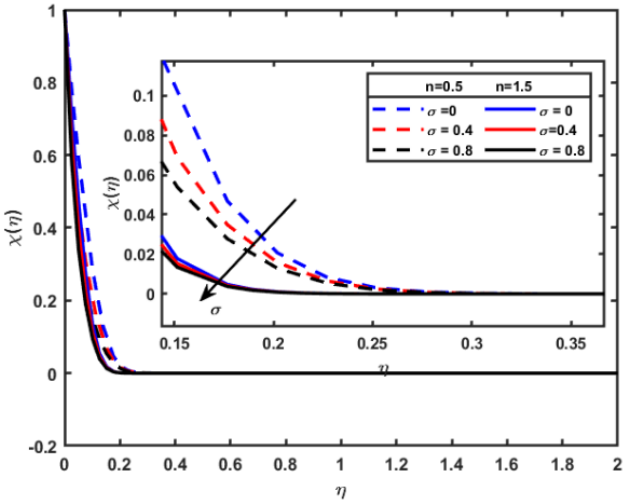

Fig. 5.4 Variation of σ on mass transfer profile

enhances mass transfer by facilitating faster diffusion of substances through a fluid medium. Higher diffusivity means particles can move more readily with less obstruction to mass transport. This increased diffusivity allows for quicker spreading of molecules and improving the overall efficiency of mass transfer processes such as diffusion. Chemical reaction parameter influences the rate at which chemical reactions occur within the fluid, which can in turn affect the concentration gradients of reactants and products. Higher values of the chemical reaction parameter can lead to faster reactions and more pronounced concentration gradients, resulting in an intensified mass transfer profile as proved in Fig 5.4.

From Table 2, it is observed that adding the MoS_2 nanoparticles to the base fluid reduces the local skin friction. In general, MoS_2 nanoparticles exhibit inherent lubricating properties which when dispersed in the ethylene glycol create a lubricious layer at the surface. Further, it weakens the friction between the fluid and the solid boundary. In addition, shear thickening fluids have shown more substantial frictional effects when compared to Newtonian and shear thinning fluids. These factors are crucial to the enhancement of the quality of the products in various applications. An enhancement in heat transfer is observed when MoS_2 nanoparticle is added to $C_2H_6O_2$. This phenomenon is primarily attributed to the unique thermal and fluid dynamic properties of these nanoparticles. The enhanced thermal conductivity of MoS_2 promotes more efficient heat transfer, as it facilitates the transfer of heat from the solid surface to the fluid. The local heat transfer coefficient is more significant in dilatant fluids compared to Newtonian and Pseudoplastic fluids. The mass transfer coefficient is improved for nanoparticles with higher volume fraction.

Table 3 constitutes the influences of engineering parameters with variation in MoS_2 volume fraction using statistical measures. From this, it is observed that shear thickening nanofluids have substantial frictional effects compared to Newtonian and shear thinning nanofluids. The correlation between MoS_2 volume fraction and local wall friction coefficient is very strong negative and the consistency of C_{fx}, Nu_x, Sh_x is more in shear thinning fluids. The heat and mass transfer coefficients are very strong positively correlated to variation of MoS_2 volume fraction. It is noticed that, C_{fx}, Nu_x, Sh_x are more prominent in shear thickening fluids compared to other fluids (Newtonian and shear thinning). Table 3 renders that the statistical results of the engineering parameters are in close association with the numerical results.

From Table 4, it is observed that heat transfer coefficient weakens for enhanced values of variable thermal conductivity and variable mass diffusivity parameters. Shear thickening nanofluids stimulate high heat transfer phenomenon compared to Newtonian and shear thinning fluids. Mass transfer coefficient is enhanced for augmenting values of variable thermal conductivity parameter whereas for variable mass diffusivity parameter it shows a contrary nature.

Table 5 reports that there is a good agreement with the works of Khan and Shahzad in comparison of local Skin friction for distinct values of material parameter (A) and Power law index (n) for fixed values of $M=0$, $\phi=0$, $Da=0$, $P_r=0$, $R=0$, $\varepsilon = 0$, $N_T=10^{-6}$, $N_B=10^{-6}$, $\sigma=0$, $L_e=0$, $\varepsilon_1 = 0$.

Table 2 Variation of MoS_2 volume fraction on C_{fx}, Nu_x, and Sh_x

Parameter	$\frac{1}{2}Re_b^{\frac{1}{n+1}}C_{fx}$			$Re_b^{-\frac{1}{n+1}}Nu_x$			$Re_b^{-\frac{1}{n+1}}Sh_x$		
ϕ	n=0.5	n=1	n=1.5	n=0.5	n=1	n=1.5	n=0.5	n=1	n=1.5
0.0	-2.82857	-2.738911	-2.688379	8.830680	10.900430	11.975013	11.91773	13.440548	14.291137
0.01	-2.910975	-2.824571	-2.775978	9.955081	12.285956	13.496400	11.986351	13.534162	14.397428
0.02	-2.995785	-2.912719	-2.866188	11.077662	13.669586	15.015875	12.048423	13.618103	14.492449
0.03	-3.082886	-3.003300	-2.958965	12.199990	15.053214	16.535496	12.105195	13.694260	14.578459

Table 3 Statistical data analysis of C_{fx}, Nu_x, Sh_x

Statical measure	$\frac{1}{2}Re_b^{\frac{1}{n+1}}C_{fx}$			$Re_b^{-\frac{1}{n+1}}Nu_x$			$Re_b^{-\frac{1}{n+1}}Sh_x$		
	n=0.5	n=1	n=1.5	n=0.5	n=1	n=1.5	n=0.5	n=1	n=1.5
Mean	-2.954556	-2.869875	-2.82237	10.51585	12.9773	14.2557	12.01442	13.5717	14.43987
Standard deviation	0.0947895	0.09854160	0.100085	1.255609	1.547500	1.699515	0.0698804	0.094582	0.1071148
C.V	3.2082	3.4336	3.5732	11.9406	11.9252	11.9216	0.5816	0.6969	0.7417
Correlation	-0.9992	-0.99991	-0.99999	0.9999	0.9999	1	0.9990	0.9989	0.9988

Table 4 Variation of variable thermal conductivity and mass diffusivity on Nu_x, Sh_x

Parameter	$Re_b^{-\frac{1}{n+1}}Nu_x$			$Re_b^{-\frac{1}{n+1}}Sh_x$		
ε	n=0.5	n=1	n=1.5	n=0.5	n=1	n=1.5
0.05	10.307364	12.720381	13.973515	11.767799	13.260127	14.094774
0.2	9.260803	11.429694	12.555961	12.411284	14.067545	14.986729
0.6	6.746357	8.327489	9.148444	13.862629	15.897671	17.011717
ε_1						
0.05	9.99418	12.332781	13.547320	12.327948	13.913707	14.798557
0.2	9.878705	12.194384	13.396835	11.378969	12.858967	13.683699
0.8	9.460605	11.693840	12.852867	9.009009	10.219599	10.891668

Table 5 Validation of solutions for Local Skin friction compared with previous existing works

A	n	(Khan and Shahzad 2013)	Present results
1	1	-1.414214	-1.414630
	2	-1.343198	-1.343313
	3	-1.311338	-1.311145
0		-1	-1.001396
1	1	-1.414214	-1.414630
2		-1.732051	-1.734840

5. Conclusions

A The current study emphasizes the mathematical model for understanding the heat and mass transfer characteristics of MoS_2 nanoparticle suspension in ethylene glycol over a stretching sheet. To address the non- Newtonian and Newtonian flow behaviors, Sisko fluid model is taken into account. The additional effects such as MHD, variable thermal conductivity, thermal radiation, variable mass diffusivity, chemical reaction has shed light on the nanofluid-based transport phenomena. The incorporation of MoS_2 nanoparticles into the ethylene glycol base fluid has been demonstrated to enhance both heat and mass transfer rates making this nanofluid attractive for various industrial applications.

The major outcomes of the flow problem investigated in the present work are as follows:

• Fluid flow pattern: The fluid flow rate substantially declines for enhanced values nanoparticle volume fraction, magnetic field and porous permeability parameters, but it upsurges for the material parameter.

• Adding MoS_2 nanoparticles to the base fluids diminishes friction between the fluid and the solid boundary. These findings improve the lifetime and efficiency of bearings and gears in mechanical systems.

• Temperature distribution improves for enriching

parameters of volume fraction, variable thermal conductivity, mass diffusivity, Brownian and thermophoresis parameters.

• The heat transfer is obstructed for propagating the values of Prandtl number.

• Mass transfer profile proliferates for higher values of variable mass diffusion and Brownian motion parameters but shows a contrary nature for thermophoresis and chemical reaction parameters.

• The correlation between variation of MoS_2 volume fraction and local wall friction coefficient are very strong negative.

• Heat transfer coefficient enriches for higher values of MoS_2 volume fraction.

• A discernible enhancement in mass transfer coefficient is observed on amplification of nanoparticle volume fraction for dilatants fluids.

The results obtained from this investigation provide valuable insights into the design and optimization of systems involving nanofluid-based heat and mass transfer processes such as: solar collectors, chemical reactors, and heat exchangers. Furthermore, these theoretical findings contribute to an understanding of the complex interplay between variable properties and transport phenomena in nanofluid suspensions fostering further advancements in rapidly evolving field. The future work would be the focused on enhancing the stability of MoS_2 nanoparticles suspension in the $C_2H_6O_2$ using effective surfactant for more heat transfer applications by implementing more advanced methods.

Acknowledgment

The Authors would like to thank Dr. C.S Ramesh, Dean R& D for giving their valuable insights and a special thanks to anonymous reviewers for their critical and educative comments which helped to improve the quality of the manuscript.

References

Abd-Elkader, O.H., Abdelsalam, H., Sakr, M.A., Shaltout, A.A. and Zhang, Q. (2023), "First-principles study of MoS_2, WS_2, and NbS_2 quantum dots: Electronic properties and hydrogen evolution reaction", *Crystals*, **13**(7), 994. https://doi.org/10.3390/cryst13070994.

Ahmed Abdalglil Mustafa, W., Dassenoy, F., Sarno, M. and Senatore, A. (2022), "A review on potentials and challenges of nanolubricants as promising lubricants for electric vehicles", *Lubr. Sci.*, **34**(1), 1-29. https://doi.org/10.1002/ls.1568.

Algehyne, E.A., Alrihieli, H.F., Bilal, M., Saeed, A. and Weera, W. (2022), "Numerical approach toward ternary hybrid nanofluid flow using variable diffusion and non-Fourier's concept", *ACS Omega*, **7**(33), 29380-29390. https://doi.org/10.1021/acsomega.2c03634.

Ali, B., Ahammad, N.A., Awan, A.U., Guedri, K., Tag-ElDin, E. M. and Majeed, S. (2022), "Dynamics of rotating micropolar fluid over a stretch surface: the case of linear and quadratic convection significance in thermal management", *Nanomaterials*, **12**(18), 3100. https://doi.org/10.3390/nano12183100.

Alsenafi, A., Bég, O.A., Ferdows, M., Bég, T.A. and Kadir, A. (2021), "Numerical study of nano-biofilm stagnation flow from a nonlinear stretching/shrinking surface with variable nanofluid and bioconvection transport properties", *Sci. Rep.*, **11**(1), 9877. https://doi.org/10.1038/s41598-021-88935-9

Amirsom, N.A., Uddin, M.J., Md Basir, M.F., Kadir, A., Bég, O.A. and Md. Ismail, A.I. (2019), "Computation of melting dissipative magnetohydrodynamic nanofluid bioconvection with second-order slip and variable thermophysical properties", *Appl. Sci.*, **9**(12), 2493. https://doi.org/10.3390/app9122493.

Awan, A.U., Ahammad, N.A., Shatanawi, W., Allahyani, S.A., Tag-ElDin, E.M., Abbas, N. and Ali, B. (2022), "Significance of magnetic field and Darcy–Forchheimer law on dynamics of Casson-Sutterby nanofluid subject to a stretching circular cylinder", *Int. Commun. Heat Mass Transf.*, **139**, 106399. https://doi.org/10.1016/j.icheatmasstransfer.2022.106399.

Awan, A.U., Shah, S.A.A. and Ali, B. (2022), "Bio-convection effects on Williamson nanofluid flow with exponential heat source and motile microorganism over a stretching sheet", *Chin. J. Phys.*, **77**, 2795-2810. https://doi.org/10.1016/j.cjph.2022.04.002.

Bazaka, K., Levchenko, I., Lim, J.W.M., Baranov, O., Corbella, C., Xu, S. and Keidar, M. (2019), "MoS_2-based nanostructures: synthesis and applications in medicine", *J. Phys D: Appl. Phys.*, **52**(18), 183001. https://doi.org/10.1088/1361-6463/ab03b3.

Bas, H. (2023), "Tribological properties of MoS2 particles as lubricant additive on the performance of statically loaded radial journal bearings," *Turk. J. Eng.*, **7**(1), 42-48. https://doi.org/10.31127/tuje.1016153.

Bisht, A., and Maheshwari, S. (2023). "Magnetized Sisko nanofluid flow over nonlinear stretching sheet: A computational approach", *Numer. Heat Tr. A: Appl.*, 1-21. https://doi.org/10.1080/10407782.2023.2242613

Choi, S.U.S. and Eastman, J.A. (1995), "Enhancing thermal conductivity of fluids with nanoparticles", *Int. Mech. Eng. Cong. Exhibition*, San Francisco, United States, November.

Choudhary, R. and Jain, S. (2021), "Temperature jump and concentration slip effects on bioconvection past a vertical porous plate in the existence of nanoparticles and gyrotactic microorganism with inclined MHD", *Adv. Nano. Res.*, **11**(1), 27-36. https://doi.org/10.12989/anr.2021.11.1.027.

Cui, J., Jan, A., Farooq, U., Hussain, M. and Khan, W.A. (2022), "Thermal analysis of radiative Darcy–Forchheimer nanofluid flow across an inclined stretching surface", *Nanomaterials*, **12**(23), 4291. https://doi.org/10.3390/nano12234291.

Cui, J., Munir, S., Raies, S.F., Farooq, U., & Razzaq, R. (2022), "Non-similar aspects of heat generation in bioconvection from flat surface subjected to chemically reactive stagnation point flow of Oldroyd-B fluid", *Alexandria Eng. J.*, **61**(7), 5397-5411.

Ganesh, N.V., Al-Mdallal, Q.M. and Kameswaran, P.K. (2019), "Numerical study of MHD effective Prandtl number boundary layer flow of γ Al_2O_3 nanofluids past a melting surface", *Case Stud. Therm. Eng.*, **13**, 100413. https://doi.org/10.1016/j.csite.2019.100413.

Gharsseldien, Z.M. and Awaad, A. S. (2022), "Maxwell nanofluid flow through a heated vertical channel with peristalsis and magnetic field", *Adv. Nano Res.*, **13**(1), 77-86. https://doi.org/10.12989/anr.2022.13.1.077.

Hamid, A., Naveen Kumar, R., Punith Gowda, R.J., Varun Kumar, R.S., Khan, S.U., Ijaz Khan, M. and Muhammad, T. (2021), "Impact of Hall current and homogenous–heterogenous reactions on MHD flow of GO-MoS_2/water (H_2O)-ethylene glycol ($C_2H_6O_2$) hybrid nanofluid past a vertical stretching surface", *Waves Random Complex Media*, 1-18. https://doi.org/10.1080/17455030.2021.1985746.

Huang, X., Shan, H., Chu, W. and Chen, Y. (2022), "Computational and mathematical simulation for the size-dependent dynamic behavior of the high-order FG nanotubes, including the porosity under the thermal effects", *Adv. Nano Res.*, **12**(1), 101-115.

https://doi.org/10.12989/anr.2022.12.1.073.

Hussain, S.M. (2022), "Dynamics of ethylene glycol-based graphene and molybdenum disulfide hybrid nanofluid over a stretchable surface with slip conditions", *Sci. Rep.*, **12**(1), 1751. https://doi.org/10.1038/s41598-022-05703-z.

Hussain, M., Sharif, H., Khadimallah, M. A., Mouldi, A., Loukil, H., Ali, M. R. and Tounsi, A. (2023), "Shooting method applied to porous rotating disk: Darcy-Forchheimer flow of nanofluid", *Adv. Nano Res.*, **14**(3), 295-302. https://doi.org/10.12989/anr.2023.14.3.295.

Jan, A., Mushtaq, M., Farooq, U. and Hussain, M. (2022), "Nonsimilar analysis of magnetized Sisko nanofluid flow subjected to heat generation/absorption and viscous dissipation", *J. Magn. Magn.*, **564**, 170153. https://doi.org/10.1016/j.jmmm.2022.170153.

Khan, M. and Shahzad, A. (2013), "On boundary layer flow of a Sisko fluid over a stretching sheet", *Quaest. Math.*, **36**(1), 137-151. https://doi.org/10.2989/16073606.2013.779971.

Kobayashi, Y., Morimoto, H., Nakagawa, T., Gonda, K. and Ohuchi, N. (2013), "Preparation of silica-coated gadolinium compound particle colloid solution and its application in imaging", *Adv. Nano Res.*, **1**(3), 159-169. https://doi.org/10.12989/anr.2013.1.3.159.

Liu, M., Zhu, H., Wang, Y., Sevencan, C., and Li, B. L. (2021), "Functionalized MoS2-based nanomaterials for cancer photo-therapy and other biomedical applications", *ACS Mater. Lett.*, **3**(5), 462-496. https://doi.org/10.1021/acsmaterialslett.1c00073

Liu, X., Xu, J., Lai, T. and He, M. (2023), "Investigation on the heat transfer of MHD nanofluids in channel containing porous medium using lattice Boltzmann method", *Adv. Nano Res.*, **15**(3), 191. https://doi.org/10.12989/anr.2023.15.3.191.

Maalla, A. and Song, J. (2021), "Computational modeling for nonlinear magneto-electro-elastic responses of smart multi-phase symmetric system", *Adv. Nano Res.*, **11**(3), 327-337. https://doi.org/10.12989/anr.2021.11.3.327.

Mousavi, S.B., Heris, S.Z. and Estellé, P. (2020), "Experimental comparison between ZnO and MoS_2 nanoparticles as additives on performance of diesel oil-based nano lubricant", *Sci. Rep.*, **10**(1), 5813. https://doi.org/10.1038/s41598-020-62830-1.

Nagaraja, B., Ajaykumar, A.R., Felicita, A., Pradeep Kumar. and Rudraswamy Ng. (2023), "Non-Darcy-Forchheimer flow of Casson-Williamson nanofluid on melting curved stretching sheet influenced by magnetic dipole", *ZAMM*, **103**(10). https://doi.org/10.1002/zamm.202300134.

Pal, D. and Mandal, G. (2019), "Magnetohydrodynamic heat and mass transfer of Sisko nanofluid past a stretching sheet with nonlinear thermal radiation and convective boundary condition", *J. Nanofluids*, **8**(4). 852-860. https://doi.org/10.1166/jon.2019.1620.

Pavithra, K.M., Hanumagowda, B.N., Varma, S.V.K., Ahammad, N.A., Raju, C.S.K. and Noeiaghdam, S. (2023), "The impacts of shape factors in a chemically reacting two-passage vertical channel filled with kerosene based graphene oxide and MoS_2 mixture in a porous medium", *Results Eng.*, **18**, 101050. https://doi.org/10.1016/j.rineng.2023.101050.

Pourmadadi, M., Tajiki, A., Hosseini, S.M., Samadi, A., Abdouss, M., Daneshnia, S. and Yazdian, F. (2022), "A comprehensive review of synthesis, structure, properties, and functionalization of MoS_2; emphasis on drug delivery, photothermal therapy, and tissue engineering applications", *J. Drug Delivery Sci. Tech.*, **76,** 103767. https://doi.org/10.1016/j.jddst.2022.103767.

Raju, C.S.K. and Sandeep, N. (2016), "Heat and mass transfer in 3D non-Newtonian nano and ferro fluids over a bidirectional stretching surface", *Int. J. Eng. Res. Afr.*, **21**, 33-51. https://doi.org/10.4028/www.scientific.net/JERA.21.33

Rashed, A.S., Mahmoud, T.A. and Kassem, M.M. (2021), "Behavior of nanofluid with variable brownian and thermal diffusion coefficients adjacent to a moving vertical plate", *J. Appl. Comput. Mech.*, **7**(3), 1466-1479. https://doi.org/10.22055/jacm.2021.34852.2483.

Razzaq, R., Farooq, U., Cui, J. and Muhammad, T. (2021), "Non-similar solution for magnetized flow of Maxwell nanofluid over an exponentially stretching surface", *Math. Probl. Eng.*, **2021**, 1-10. https://doi.org/10.1155/2021/5539542.

Razzaq, R. and Farooq, U. (2021), "Non-similar forced convection analysis of Oldroyd-B fluid flow over an exponentially stretching surface", *Adv. Mech. Eng.*, **13**(7), 16878140211034604.

Rosseland S, (1931), *Astrophysik und Atom-Theoretische Grundlagen*, Springer, Berlin, Germany, 41-44.

Saidi, M.Z., El Moujahid, C., Pasc, A., Canilho, N., Delgado-Sanchez, C., Celzard, A. and Chafik, T. (2021), "Enhanced tribological properties of wind turbine engine oil formulated with flower-shaped MoS_2 nano-additives", *Colloids Surf. A.*, **620**, 126509. https://doi.org/10.1016/j.colsurfa.2021.126509.

Safari, M., Mohammadimehr, M. and Ashrafi, H. (2021), "Free vibration of electro-magneto-thermo sandwich Timoshenko beam made of porous core and GPLRC", *Adv. Nano Res.*, **10**(2), 115-128. https://doi.org/10.12989/anr.2021.10.2.115.

Selmi, A. (2019) "Effectiveness of SWNT in reducing the crack effect on the dynamic behavior of aluminium alloy", *Adv. Nano Res.*, **7**(5), 365-377. https://doi.org/10.12989/anr.2019.7.5.365.

Shah, S.A.A., Ahammad, N.A., Ali, B., Guedri, K., Awan, A.U., Gamaoun, F. and Tag-ElDin, E.M. (2022), "Significance of bio-convection, MHD, thermal radiation and activation energy across Prandtl nanofluid flow: A case of stretching cylinder", *Int. Commun. Heat Mass Transf.*, **137**, 106299. https://doi.org/10.1016/j.icheatmasstransfer.2022.106299.

Shah, S.A.A., Ahammad, N.A., Din, E.M.T.E., Gamaoun, F., Awan, A.U. and Ali, B. (2022), "Bio-convection effects on prandtl hybrid nanofluid flow with chemical reaction and motile microorganism over a stretching sheet", *Nanomaterials*, **12**(13), 2174. https://doi.org/10.3390/nano12132174.

Shah, S.A.A. and Awan, A.U. (2022), "Significance of magnetized Darcy-Forchheimer stratified rotating Williamson hybrid nanofluid flow: A case of 3D sheet", *Int. Commun. Heat Mass Transf.*, **136**, 106214. https://doi.org/10.1016/j.icheatmasstransfer.2022.106214.

Sharif, H., Khadimallah, M.A., Naeem, M.N., Hussain, M., Mahmoud, S.R., Al-Basyouni, K.S. and Tounsi, A. (2021), "The investigation of Magnetohydrodynamic nanofluid flow with Arrhenius energy activation", *Adv. Nano Res.*, **10**(5), 437-448. https://doi.org/10.12989/anr.2021.10.5.437.

Sidik N.A.C, Yazid M.N.A.W.M. and Mamat R. (2015), "A review on the application of nanofluids in vehicle engine cooling system". *Int. Commun. Heat Mass Transf.*, **68**, 85-90. https://doi.org/10.1016/j.icheatmasstransfer.2015.08.017.

Sivaraj, R., Benazir, A.J., Srinivas, S. and Chamkha, A.J. (2019), "Investigation of cross-diffusion effects on Casson fluid flow in existence of variable fluid properties", *Eur. Phys. J. Spec. Top.*, **228**, 35-53. https://doi.org/10.1140/epjst/e2019-800187-3

Sohail, M., Nazir, U., Chu, Y.M., Alrabaiah, H., Al-Kouz, W. and Thounthong, P. (2020), "Computational exploration for radiative flow of Sutterby nanofluid with variable temperature-dependent thermal conductivity and diffusion coefficient", *Open Phys.*, **18**(1), 1073-1083. https://doi.org/10.1515/phys-2020-0216.

Sur, U.K. (2014), "Biological green synthesis of gold and silver nanoparticles", *Adv. Nano. Res.*, **2**(3), 135-145. https://doi.org/10.12989/anr.2014.2.3.135.

Waqas, H., Farooq, U., Muhammad, T. and Manzoor, U. (2022), "Importance of shape factor in Sisko nanofluid flow considering gold nanoparticles", *Alex. Eng. J.*, **61**(5), 3665-3672. https://doi.org/10.1016/j.aej.2021.09.010.

Zhang, Y., Li, C., Jia, D., Zhang, D. and Zhang, X. (2015), "Experimental evaluation of the lubrication performance of

MoS2/CNT nanofluid for minimal quantity lubrication in Ni-based alloy grinding", *Int. J. Mach. Tools and Manuf.*, **99**, 19-33. https://doi.org/10.1016/j.ijmachtools.2015.09.003.

CC

Nomenclature

A	Sisko fluid parameter/material parameter.
a_{nf}	Shear rate viscosity/ dynamic viscosity of nanofluid ($kgm^{-1}s^{-1}$).
b	Consistency index of Sisko nanofluid (Pa s^{n-2})
B_0	Magnetic induction parameter (A/m)
Cp	Specific heat capacity at constant pressure (J/KgK)
C	Concentration (Kg/m^3).
C_w	Nanoparticles wall concentration (Kg/m^3).
$C\infty$	Ambient concentration (Kg/m^3).
C_{fx}	Skin friction coefficient
D_T	Thermophoretic motion coefficient (m^2/s).
D_B	Brownian motion coefficient (m^2/s).
f	Dimensionless velocity.
K	Permeability parameter (m^2).
μ_{anf}	Dynamic viscosity of the nanofluid (Ns/m^2).
K_r	Chemical reaction parameter (s^{-1}).
K^*	Mean absorption Coefficient.
k_{nf}	Thermal conductivity of the nanoparticle(W/mK).
k_f	Thermal conductivity of the base fluid(W/mK).
M	Magnetic field parameter
n	Power law index
N_B	Dimensionless Brownian motion parameter
N_T	Dimensionless Thermophoresis parameter
Nu_x	Local Nusselt number
P_r	Prandtl number
q_r	Radiative heat flux(W/m^2)
R	Thermal radiation
Re	Reynolds number
Sh_x	Local Sherwood number
T	Temperature of the fluid (K).
$T\infty$	Ambient temperature(K).
T_w	Wall temperature(K).
u, v	Velocity components in *x*, *y* directions respectively (m/s)
x	Distance along the surface (m)
y	Distance perpendicular to the surface (m)
σ	Dimensionless chemical reaction parameter.
D_a	Dimensionless porous medium parameter.
τ	Ratio between the effective heat capacitance the nano-particle material and heat capacitance of the fluid.
ε	Variable thermal conductivity parameter
ε_1	Variable mass diffusivity parameter
χ	Dimensionless concentration.
θ	Dimensionless temperature.
α	Thermal diffusion coefficient(m^2/s).